2014 International Microwave Symposium, June 2014 (to appear).

Transmission-Line-Based Multi-Way Lossless Power Combining and Outphasing System

Taylor W. Barton, Alexander S. Jurkov, and David J. Perreault
Massachusetts Institute of Technology, Cambridge, MA 02139

***Abstract*—This paper presents a non-isolating multi-way outphasing and power combining system that achieves nearly resistive loading of branch amplifiers over the entire output power range through a combiner network comprising only transmission line sections. We derive a design methodology and describe an outphasing control law that selects control angles to minimize the peak susceptive loading of the branch PAs over a specified output power range. The approach is demonstrated in a 2.14-GHz, four-way outphasing amplifier system that achieves >60% drain efficiency over a 6.2-dB output power range.**

***Index Terms*—base stations, outphasing, power amplifier (PA), wideband code division multiple access (W-CDMA), Chireix, LINC, load modulation.**

I. Introduction

Power amplifiers (PAs) employed in many RF applications are required to provide dynamic control of their output power over a wide range while maintaining high efficiency. One promising strategy to achieve high overall system efficiency with modulated signals is to employ saturated or switched-mode PAs in an outphasing architecture. Chireix outphasing is an example of this technique, in which multiple "branch" PAs interact via the combining network such that variations in relative phase among the branch PAs causes the effective impedance seen by each branch PA to change, modulating the total output power. A drawback of the Chireix technique is the significant variable reactive loading of the branch PAs that occurs across the outphasing (power) range.

A power combining and outphasing system that provides ideally lossless power combining, along with nearly resistive branch PA loading over a very wide output power range has recently been introduced [1], [2]. The performance of this power combining architecture, which combines power from four or more outphasing PAs, has so far been experimentally demonstrated for lumped-element-based implementations [2], [3], and with microstrip-based structures that incorporate reactive elements in a shunt connection to ground [4]. At sufficiently high frequencies, however, the quality of discrete passive components can significantly degrade, and accuracy of component values and repeatability of component placement become challenging issues. Furthermore, it may be advantageous to realize the combining network using only power-path transmission line sections, in order to limit the effects of ground return paths and stub parasitics. In this work, we present a new multi-way power combining network that is related to that in [1] but that is composed entirely of transmission line sections connected in a tree structure. This approach shares the benefits of some Chireix-like transmission-line combiners [5], [6] but provides greatly reduced reactive loading of the power amplifiers across the outphasing range. A four-branch prototype amplifier system operating at 2.14 GHz and over 100 W peak power demonstrates the proposed architecture.

II. Power Combining Network

The proposed four-way transmission-line (TL) power combiner is shown in Fig. 1. (Higher-order versions can be realized by direct extension, but we focus on the four-way implementation as having a combination of high performance and widespread applicability.) The transmission lines have characteristic impedance Z_1 and Z_2. Each transmission line is selected as having a length that is a specified offset from a base length. That is, the transmission-line lengths are defined as a particular increment/decrement (Δ_1 or Δ_2) from a base length (e.g., a half-wavelength). This methodology for sizing the transmission lines allows for design symmetry and greatly simplifies the analysis of the combiner. A quarter-wavelength ($\ell_{\text{base}} = \lambda/4$) is the shortest possible TL base length that will allow for desired operation with symmetric length increments $\pm\Delta_{1,2}$. A half-wavelength base length — selected for the example design here — may also be used, and half wavelength increments may be added to the base transmission line lengths without changing the operating characteristics, but shorter lengths are preferable when possible because of loss considerations. The example design presented here utilizes a half wavelength TL base length as it results in TL lengths compatible with practical layout and the physical dimensions of the branch PAs.

A. Design Methodology

The design of the TL combiner of Fig. 1 begins with a specification on its operating output power range and its load resistance R_L. In general, Z_1 and Z_2 are selected to be larger (2x – 10x) than the specified load resistance R_L for which the combiner is designed. Larger values of Z_1 and Z_2 with respect to R_L result in smaller branch PA loading susceptance variations with output power control and narrower output power range (over which the combiner is optimized to operate). On the other hand, smaller values of Z_1 and Z_2 with respect to R_L result in wider operating power range at the cost of larger branch PA susceptive load variation. Note that physical implementability limits how large one can select Z_1 and Z_2 to be.

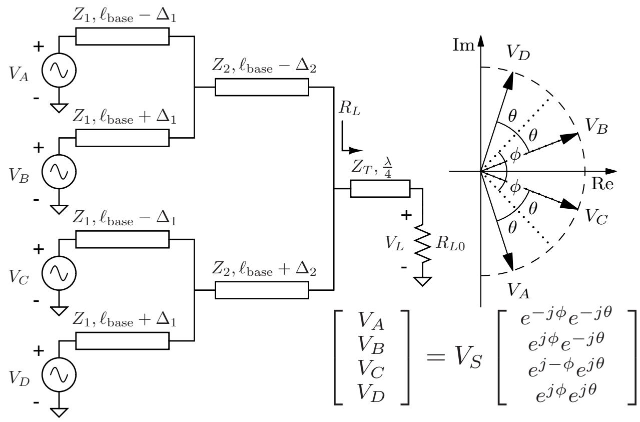

Fig. 1. Four-way power combiner implementation using all transmission line elements, with phasor relationship of the four PA input voltages. The base length ℓ_{base} may be selected as a quarter wavelength or any multiple, with R_L, Z_1, Z_2, Δ_1, and Δ_2 as design variables. The quarter-wave line Z_T provides an impedance transformation between a design impedance R_L and an actual desired load impedance R_{L0}. The branch PAs are represented as ideal voltage sources.

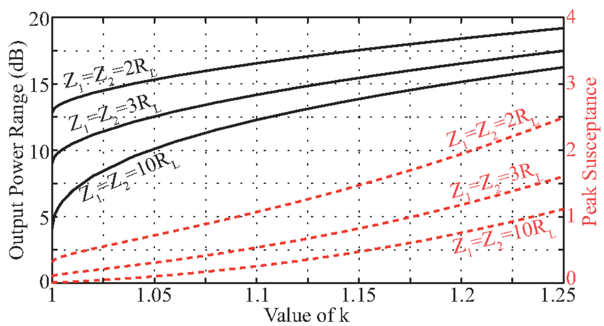

Fig. 2. Design curves for the four-way TL combiner for TL characteristic impedances Z_1 and Z_2 of 2x, 3x, and 10x the load resistance R_L. The susceptance axis is normalized to a combiner load $R_L = 1\Omega$; to denormalize, multiply axis by $1/R_L$.

A design parameter k that uniquely characterizes the combiner is selected based on the intended combiner operating power range. To aid in the selection of the appropriate value for k, a set of design curves are shown in Fig. 2 for the TL combiner for various transmission-line characteristic impedances. To determine the necessary value of k for a particular TL combiner operating output power range, start from the left Output Power Range axis and trace the desired power range to a black curve corresponding to the selected transmission-line characteristic impedances Z_1 and Z_2. Tracing then vertically down to the k-value axis yields the appropriate value of k. The resultant peak susceptive PA loading (normalized to $1/R_L$) for the chosen value of k is then given by tracing the k value vertically up to a red curve corresponding to the values of Z_1 and Z_2, and then tracing horizontally (right) to the Peak Susceptance axis. The design curves in Fig. 2 are generated for transmission lines having identical characteristic impedances, which may result in certain simplifications to the construction of the combiner. However, similar design curves can be generated for any arbitrary combination of Z_1 and Z_2.

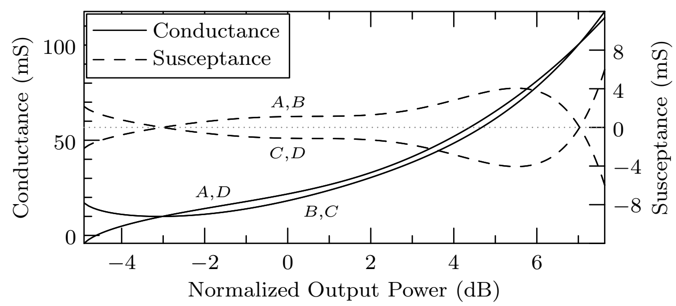

Fig. 3. Effective loading impedance seen by each branch PA driving the four-way TL combiner of Fig. 1 with $Z_1 = Z_2 = 100\ \Omega$, $\ell_{\text{base}} = \lambda/2$, $\Delta_1 = 0.201\lambda$ and $\Delta_2 = 0.196\lambda$, $Z_T = 40.8\ \Omega$ and $R_{L0} = 50\ \Omega$ as a result of the OS outphasing control law. (R_L for this design is 33.3 Ω). Power is normalized to that of all four PAs driving 50-Ω loads.

Once the value of k is selected for a particular output power range along with a set of transmission-line characteristic impedances Z_1 and Z_2, the transmission-line length increments Δ_1 and Δ_2 can be computed according to (1)-(2) for the $\lambda/2$ base-length combiner. For the $\lambda/4$ base-length combiner, the inverse sine functions are replaced with inverse cosine functions.

$$\Delta_1 = \frac{\lambda}{2\pi} \sin^{-1}\left(\frac{2R_L}{(k+1)(k+Z_1\sqrt{k^2-1})}\right) \tag{1}$$

$$\Delta_2 = \frac{\lambda}{2\pi} \sin^{-1}\left(\frac{2R_L}{(k+1)Z_2}\right) \tag{2}$$

Although the main portion of the combiner network is designed around a particular load resistance R_L, an optional impedance transformation stage (implemented as a final quarter-wave line with impedance Z_T in Fig. 1) may be provided to transform between the design resistance R_L and an actual load resistance R_{L0}. (The final impedance transformation can optionally be eliminated, or implemented through other means, such as a matching network or transmission-line transformer.) Including this final impedance transformation provides greater design flexibility and allows one to design the combiner network without requiring transmission lines with high characteristic impedances.

B. Control Law

With all four branch PAs operating simultaneously with equal amplitudes V_S and the phasor relationship indicated in Fig. 1, output power control can achieved by modulation of the outphasing angles (θ and ϕ). Transmission-line analysis shows that for the half-wavelength base line length implementation, output power is related to θ and ϕ as

$$P_{\text{out}} = \frac{8R_L V_S^2}{Z_1^2 \sin^2(\sigma_1)\cos^2(\sigma_2)} \sin^2(\phi)\cos^2(\theta) \tag{3}$$

where $\sigma_1 = 2\pi\Delta_1/\lambda$ and $\sigma_2 = 2\pi\Delta_2/\lambda$. A net phase can be applied to the output by adding a phase offset to all four of the inputs V_A–V_D.

Although an infinite number of control strategies are possible, we can select a control law based on achieving desirable

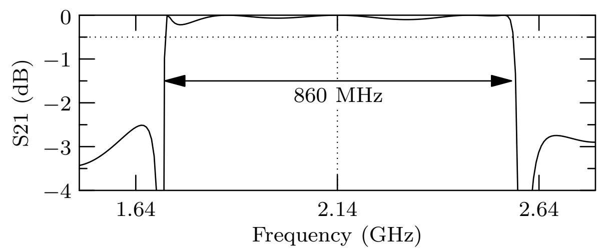

Fig. 4. The simulated combiner operating bandwidth in a back-to-back configuration is found to be 860 MHz, sufficient for many practical applications.

loading conditions for the branch amplifiers. We propose an optimal susceptance (OS) control law that selects the control angles such that the peak susceptive loading of the branch PAs over a specified output power operating range is minimized. Derived from the output power relation (3), this control law can be written (for the half-wavelength base combiner) as:

$$\phi = \arctan\left(\frac{Z_1 \tan\sigma_1 P_{\text{out}}}{2V_S^2}\right) \tag{4}$$

$$\theta = \arccos\left(\cos\sigma_2 \cos\sigma_1 \sqrt{\frac{4Vs^2 + P_{\text{out}}^2 Z_1^2 \tan^2\sigma_1}{8R_L V_S^2 P_{\text{out}}}}\right) \tag{5}$$

The resulting loading conditions for the four branch PAs is shown in Fig. 3 for an example design.

C. Operating Bandwidth

The combiner RF operating bandwidth can be characterized by an ac sweep of the transmission coefficient of a back-to-back pair of networks, with one network acting as a splitter to provide phase-shifted inputs to the combining network. The simulated results for this configuration are shown in Fig. 4. The -0.5 dB bandwidth is found to be 860 MHz (or 40%), sufficient for many practical applications.

III. Combiner Implementation

The prototype combiner design is based on the values $Z_1 = Z_2 = 100\ \Omega$, $\ell_{\text{base}} = \lambda/2$, $\Delta_1 = 0.201\lambda$ and $\Delta_2 = 0.196\lambda$. The design resistance R_L of 33.3 Ω is matched to the desired 50 Ω load (R_{L0}) by choosing $Z_T = 40.8\ \Omega$. For the Rogers RO4350 substrate, a 60-mil substrate thickness results in practical dimensions for both the 100-Ω and 40.8-Ω characteristic impedances.

Transmission line dimensions were initially found using [7] and were input into Agilent ADS and simulated with ideal junctions to verify the operation of the combiner. Next, the microstrip lengths were adjusted in simulation to account for the three T junctions. For each T junction, it was assumed that the nonidealities of the junction are symmetric for the lengths forming the top bar of each "T," so those lengths were adjusted by equal amounts. The S-parameters of each combiner subsection were compared to the ideal values, and length adjustments were performed iteratively in simulation until a close match was reached.

The layout is further influenced by physical constraints relating to the particulars of the prototype system, including

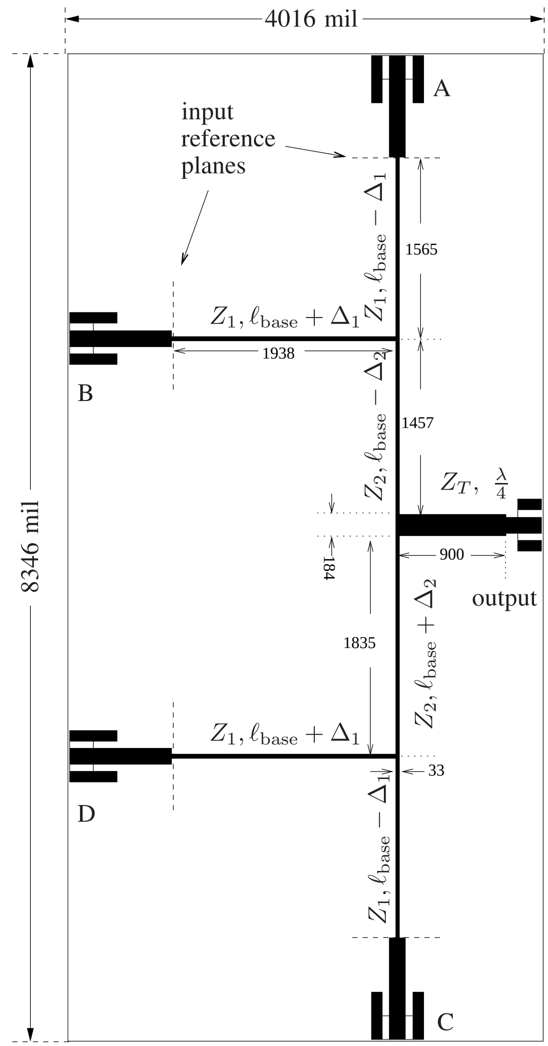

Fig. 5. Annotated final layout, with dimensions given in mils. The bottom copper layout is a solid ground plane. The board is implemented with 60-mil Rogers 4350 material.

the dimensions of the branch PAs. Interconnects are included on the combiner board to set the total electrical length between the reference plane of the combiner and that of the branch PA active devices to be an integer number of half-wavelengths. This ensures that the nearly-resistive input impedances at the combiner input are also seen by the branch PAs.

The complete layout is shown in Fig. 5. The fabricated structure was characterized by driving it in reverse, i.e. as a power splitter, and comparing the magnitude and phase of the forward voltage gains to the four 50-Ω terminated input ports. The port magnitude match was found to be within ±5% of an ideal (even) split, and the measured phase relationship is within 3 degrees of the desired values.

IV. Measured Performance

A photograph showing the RF power stage of the prototype four-way outphasing system is shown in Fig. 6. The system was characterized using the same setup as in [4], including

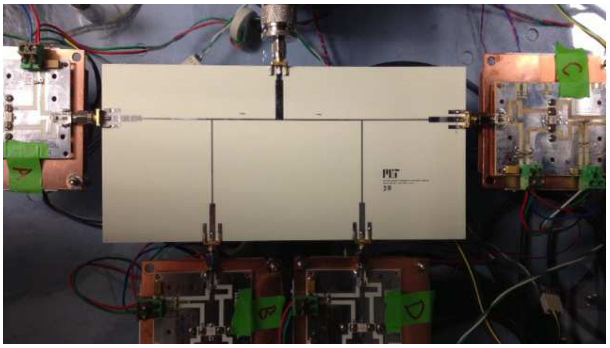

Fig. 6. Photograph of the RF power stage of the outphasing system, designed for 100 W peak at 2.14 GHz. The PAs are inverse class-F PAs suitable for load modulation based on the design in [8]. The combiner has a base length $\ell_{\text{base}} = \lambda/2$, $Z_1 = Z_2 = 100\ \Omega$, $\Delta_1 = 0.201\lambda$, $\Delta_2 = 0.196\lambda$, and $Z_T = 40.8\ \Omega$. The final-stage branch PAs and transmission-line-based power combiner are shown. Physical dimensions are detailed in Fig. 5.

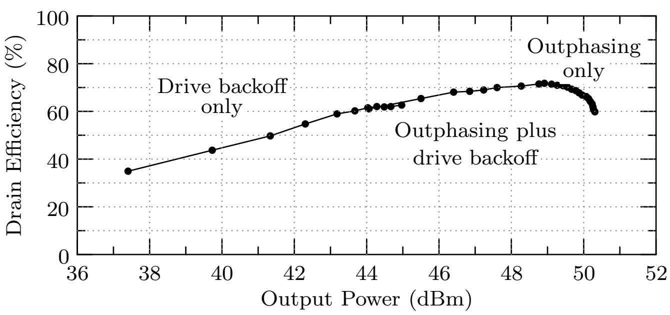

Fig. 7. CW outphasing measurements of the power amplifier system using the radial stub combining network.

four inverse class F PAs based on the design in [8] and operated with 28 V drain supply voltage as characterized in [4]. Three regions of operation are used in the outphasing sweep shown in Fig. 7. In the highest power range, pure outphasing is used for output power control, with the input power from the driver chain sufficient to saturate the branch PAs. At mid-range, the branch PA input power is modulated in addition to the outphasing control, with input power modulation used to avoid over-driving the (still saturated) branch PAs. Below the approximately 7-dB outphasing operating range, the phases of the four inputs are held constant and drive amplitude modulation is used to extend the range of output power levels, in particular enabling zero crossings of the transmitted signal. The system's modulated performance was characterized using a 3.84-MHz W-CDMA signal with 9.15-dB peak-to-average power ratio, and was measured to have an average drain efficiency of 54.5% under these conditions. Although a direct performance comparison between works is complicated by different power levels and signal PAPR, the performance of this amplifier implementation is at least on par with other state of the art amplifiers, as summarized in Table I.

V. Conclusion

We present a new multi-way lossless power combiner and outphasing system that provides highly resistive branch PA loading. This new system is based on a tree of transmission-line sections, making it highly effective for microstrip-based power amplifier systems. A complete design methodology for the combining network based on a specified output power range and load resistance is described, along with a control strategy that selects control angles to minimize the peak susceptive loading of the branch PAs over a specified output power range. The theoretical development of the approach and implementation of a 2.14-GHz, 100-W prototype system demonstrating high performance on par with the state of the art are described.

TABLE I
Comparison to other works: W-CDMA performance

Ref.	Arch.	Carrier (MHz)	P_{max} (W)	PAPR (dB)	$ACLR_1$ (dBc)	Drain Eff.
[9]	Chireix	2300	70	9.6	-49	53.5%
[10]	Chireix	2140	90	9.6	-47	50.5%
[11]	Chireix	1950	19	9.6	-47	54.5%
[8]	4-way Doherty	2140	100	6.5	-31*	61%
[3]	4-way Discrete	2140	50	3.47	-36.6	57%
[4]	4-way Hybrid	2140	48	9.6	-33	38%
This Work	4-way TL	2140	105	9.15	-34.2	54.5%

* no predistortion

References

[1] D. Perreault, "A new power combining and outphasing modulation system for high-efficiency power amplification," *IEEE Trans. Circuits Syst. I: Reg. Papers*, vol. 58, no. 8, pp. 1713–1726, Feb. 2011.

[2] A. Jurkov, L. Roslaniec, and D. Perreault, "Lossless multiway power combining and outphasing for high-frequency resonant inverters," *IEEE Trans. Power Electron.*, vol. 29, no. 4, pp. 1894–1908, April 2014.

[3] T. W. Barton, J. L. Dawson, and D. J. Perreault, "Experimental validation of a four-way outphasing combiner for microwave power amplification," *IEEE Microw. Wireless Compon. Lett.*, vol. 23, no. 1, pp. 28–30, Jan. 2013.

[4] T. W. Barton, J. L. Dawson, and D. J. Perreault, "Four-way lossless outphasing and power combining with hybrid microstrip/discrete combiner for microwave power amplification," in *IEEE MTT-S Int. Microw. Symp. Dig.*, June 2013, pp. 1–4.

[5] I. Hakala, D. Choi, L. Gharavi, N. Kajakine, J. Koskela, and R. Kaunisto, "A 2.14-GHz Chireix outphasing transmitter," *IEEE Trans. Microw. Theory Tech.*, vol. 53, no. 6, pp. 2129–2138, June 2005.

[6] W. Gerhard and R. Knoechel, "Novel transmission line combiner for highly efficient outphasing RF power amplifiers," in *Microwave Conference, 2007. European*, 2007, pp. 1433 –1436.

[7] Microstrip Analysis/Synthesis Calculator, Accessed July 2013. [Online]. Available: http://wcalc.sourceforge.net/cgi-bin/microstrip.cgi

[8] A. Grebennikov, "A high-efficiency 100-W four-stage Doherty GaN HEMT power amplifier module for WCDMA systems," in *IEEE MTT-S Int. Microw. Symp. Dig.*, June 2011, pp. 1–4.

[9] D. Calvillo-Cortes, M. van der Heijden, and L. de Vreede, "A 70W package-integrated class-E Chireix outphasing RF power amplifier," in *IEEE MTT-S Int. Microw. Symp. Dig.*, June 2013, pp. 1–3.

[10] J. Qureshi, M. Pelk, M. Marchetti, W. Neo, J. Gajadharsing, M. van der Heijden, and L. de Vreede, "A 90-W peak power GaN outphasing amplifier with optimum input signal conditioning," *IEEE Trans. Microw. Theory Tech.*, vol. 57, no. 8, pp. 1925–1935, Aug. 2009.

[11] M. van der Heijden, M. Acar, J. Vromans, and D. Calvillo-Cortes, "A 19W high-efficiency wide-band CMOS-GaN class-E Chireix RF outphasing power amplifier," in *IEEE MTT-S Int. Microw. Symp. Dig.*, June 2011, pp. 1–4.